World Journal of

Stem Cells

WJSC
World Journal of Stem Cells

Contents

Contents

ABOUT COVER

Editorial Board Member of *World Journal of Stem Cells*, Luminita Labusca, MD, PhD, Senior Researcher, National Institute of Research and Development in Technical Physics Iasi, 47 D Mangeron Boulevard, Iasi 70050, Romania. drlluminita@yahoo.com

AIMS AND SCOPE

The primary aim of *World Journal of Stem Cells* (*WJSC*, *World J Stem Cells*) is to provide scholars and readers from various fields of stem cells with a platform to publish high-quality basic and clinical research articles and communicate their research findings online. *WJSC* publishes articles reporting research results obtained in the field of stem cell biology and regenerative medicine, related to the wide range of stem cells including embryonic stem cells, germline stem cells, tissue-specific stem cells, adult stem cells, mesenchymal stromal cells, induced pluripotent stem cells, embryonal carcinoma stem cells, hemangioblasts, lymphoid progenitor cells, *etc*.

INDEXING/ABSTRACTING

The *WJSC* is now abstracted and indexed in Science Citation Index Expanded (SCIE, also known as SciSearch®), Journal Citation Reports/Science Edition, PubMed, PubMed Central, Scopus, Biological Abstracts, BIOSIS Previews, Reference Citation Analysis, China National Knowledge Infrastructure, China Science and Technology Journal Database, and Superstar Journals Database. The 2022 Edition of Journal Citation Reports cites the 2021 impact factor (IF) for *WJSC* as 5.247; IF without journal self cites: 5.028; 5-year IF: 4.964; Journal Citation Indicator: 0.56; Ranking: 12 among 29 journals in cell and tissue engineering; Quartile category: Q2; Ranking: 86 among 194 journals in cell biology; and Quartile category: Q2. The *WJSC*'s CiteScore for 2021 is 5.1 and Scopus CiteScore rank 2021: Histology is 17/61; Genetics is 145/335; Genetics (clinical) is 42/86; Molecular Biology is 221/386; Cell Biology is 164/274.

RESPONSIBLE EDITORS FOR THIS ISSUE

Production Editor: *Xiang-Di Zhang*; **Production Department Director:** *Xu Guo*; **Editorial Office Director:** *Jia-Ru Fan*.

Single cell RNA sequencing reveals mesenchymal heterogeneity and critical functions of *Cd271* in tooth development

Yan-Yan Zhang, Feng Li, Xiao-Ke Zeng, Yan-Hui Zou, Bing-Bing Zhu, Jia-Jia Ye, Yun-Xiao Zhang, Qiu Jin, Xin Nie

Yan-Yan Zhang, Feng Li, Xiao-Ke Zeng, Yan-Hui Zou, Bing-Bing Zhu, Jia-Jia Ye, Yun-Xiao Zhang, Qiu Jin, Xin Nie, School & Hospital of Stomatology, Wenzhou Medical University, Wenzhou 325027, Zhejiang Province, China

Corresponding author: Xin Nie, PhD, Professor, School & Hospital of Stomatology, Wenzhou Medical University, Xueyuan West Road, Lucheng District, Wenzhou 325027, Zhejiang Province, China. dr.xinnie@qq.com

Abstract

BACKGROUND
Accumulating evidence suggests that the maxillary process, to which cranial crest cells migrate, is essential to tooth development. Emerging studies indicate that *Cd271* plays an essential role in odontogenesis. However, the underlying mechanisms have yet to be elucidated.

AIM
To establish the functionally heterogeneous population in the maxillary process, elucidate the effects of *Cd271* deficiency on gene expression differences.

METHODS
p75NTR knockout (*Cd271⁻/⁻*) mice (from American Jackson laboratory) were used to collect the maxillofacial process tissue of p75NTR knockout mice, and the wild-type maxillofacial process of the same pregnant mouse wild was used as control. After single cell suspension, the cDNA was prepared by loading the single cell suspension into the 10x Genomics Chromium system to be sequenced by NovaSeq6000 sequencing system. Finally, the sequencing data in Fastq format were obtained. The FastQC software is used to evaluate the quality of data and CellRanger analyzed the data. The gene expression matrix is read by R software, and Seurat is used to control and standardize the data, reduce the dimension and cluster. We search for marker genes for subgroup annotation by consulting literature and database; explore the effect of p75NTR knockout on mesenchymal stem cells (MSCs) gene expression and cell proportion by cell subgrouping, differential gene analysis, enrichment analysis and protein-protein interaction network analysis; understand the interaction between MSCs cells and the differentiation trajectory and gene change characteristics of p75NTR knockout MSCs by cell communication analysis and pseudo-time analysis. Last we verified the findings

single cell sequencing *in vitro*.

RESULTS

We identified 21 cell clusters, and we re-clustered these into three subclusters. Importantly, we revealed the cell–cell communication networks between clusters. We clarified that *Cd271* was significantly associated with the regulation of mineralization.

CONCLUSION

This study provides comprehensive mechanistic insights into the maxillary- process-derived MSCs and demonstrates that *Cd271* is significantly associated with the odontogenesis in mesenchymal populations.

Key Words: *Cd271*; Mesenchymal stem cells; Single cell RNA sequencing; Osteogenesis; Mineralization; Tooth development

Core Tip: Our study reveals the following findings: (1) High cellular heterogeneity and molecular details; (2) Significant functional and signaling differences between cell types; (3) Novel subclusters of mesenchymal stem cells; and (4) Crucial cell-cell interactions of mesenchymal subpopulations. We provided new insights into the biological features of mesenchymal stem cells at the single cell level. Our findings contribute to thorough exploration of the mechanism of *Cd271* in regulating odontogenesis and osteogenesis which add to the theory of tooth development.

INTRODUCTION

During the early stage of embryogenesis, cranial neural crest cells migrate throughout the maxillary and mandibular processes, which are defined as ecto-mesenchymal stem cells (MSCs)[1,2]. Ecto-MSCs were regarded as the primitive dental cells in the classical theory of tooth development. To date, in-depth studies of the odontogenesis and osteogenesis of MSCs are still lacking.

Cd271 (low-affinity nerve growth factor receptor, p75 neurotrophic receptor) is a member of the tumor necrosis factor receptor superfamily, and is implicated in various biological functions[3]. It is used as a specific cell surface marker for purifying and identifying MSCs[4]. Previous studies focused on cellular physiological functions in processes, such as migration, proliferation, differentiation, survival and apoptosis[5-8]. *Cd271* is involved in the regulation of morphogenesis and the development of various tissues, including nerves, fat, liver and teeth[9-13]. In addition to these features, emerging studies indicate that *Cd271* plays a critical role in initiating tooth development, differentiation and mineralization of odontogenic stem cells. Mitsiadis *et al*[14] indicated that *Cd271* surrounded the developing tooth germ within nerve fibers and was highly expressed in the epithelium and mesenchyme in the early stages of odontogenesis within the cells of origin[14]. The spatial–temporal expression of *Cd271* was similar to the mineralization factor *Runx2* during the early development of tooth germ[15], which was supported by other studies[16,17]. These studies indicate that *Cd271* is involved in the physiological processes of tooth development and biomineralization. However, the molecular mechanisms of *Cd271*, as a transmembrane signaling molecule, in the morphogenesis and development of teeth remains largely unknown.

Conventionally, MSCs were considered a unified group of fusiform cells. Nevertheless, accumulating evidence suggests that MSCs are functionally and morphologically heterogeneous in essence[18,19]. High-throughput single cell RNA sequencing (scRNA-Seq) is powerful for disclosing the complexity and diversity of cells and relationships among genes involved in tissues, and offers an opportunity to explore unbiased gene expression profiling of cells[20]. scRNA-Seq also provides insights into specific changes in cell lineages, trajectory inference, and the identification of biomarkers[21,22]. scRNA-seq has been used to study MSCs derived from adipose tissue, bone marrow, endometrium, placenta and dental pulp[23-27]. However, application of scRNA-seq in maxillary-process-derived MSCs is still absent.

Herein, we used the maxillary process from mouse embryos as a model to understand the development of maxillary-process-derived MSCs. We applied scRNA-Seq analysis to elucidate the cellular heterogeneity and explore molecular details better compared with conventional methods. Our study provides novel insights into the biological features of MSCs at the single cell level and the mechanism of *Cd271* in regulating odontogenesis and osteogenesis.

MATERIALS AND METHODS

Animal preparation and tissues dissection

Cd271 knockout (*Cd271$^{-/-}$*) and wild-type (*Cd271 $^{+/+}$*) mice were used in this study. The *Cd271$^{-/-}$* mice were gifts from The Jackson Laboratory (Bar Harbor, ME, United States). These mutant mice that exhibit the targeted deletion of exon III of the *Cd271* locus do not express functional full-length *Cd271*. All animal experiments were performed according to the protocols approved by the Medical Ethics Committee of Wenzhou Medical University (No. wydw2019-0224). We completed experimental steps under ethical guidelines. The animal protocol was designed to minimize pain or discomfort to the animals. The animals were housed to laboratory conditions (23 °C, 12 h/12 h light/dark, 50% humidity, ad libitum access to food and water) prior to experimentation. The homozygotes of *Cd271 $^{+/+}$* and *Cd271$^{-/-}$* mice were mated to produce heterozygous offspring. The heterozygous mice were mated to generate three types of genotype embryos, *Cd271$^{+/+}$* and *Cd271$^{-/-}$*and *Cd271$^{+/-}$*. We obtained embryos through abdominal surgery, and chose homozygous embryos from embryonic day 16.5. The embryos were placed in a 6-cm Petri dish and washed with Phosphate buffer saline (PBS). We cut the amniotic membrane with ophthalmic scissors to separate the fetal mice and washed them with PBS again. After cutting the head of the fetus, we cut the maxillary process tissue under a stereomicroscope. After the removal of nonpurpose tissues like blood stains and fatty layers, we rinsed the tissue twice in PBS. The genotype of wild-type and *Cd271* knockout mice was confirmed with a one-step genotyping kit (Vazyme, Nanjing, China).

Single cell isolation and library preparation

Maxillary processes were dissociated into single cells in dissociation solution (0.35% collagenase IV5, 2 mg/mL papain, and 120 U/mL DNase I) in 37 °C water bath with shaking for 20 min at 100 rpm. Single cell suspensions were washed and resuspended to load to the 10X Chromium platform. More than 25000 single cells were captured and subjected to 10X Chromium Controller machine to generate gel beads-in-emulsion (GEMs). mRNA was prepared using the 10X Genomics Chromium Single Cell 3′ Reagent Kit V2 (10X Genomics, Pleasanton, CA, United States). Cells were divided by partitions into the GEMs along with GelBeads coated with oligos in this step. These oligos utilized poly-dT sequences to capture mRNAs and cell-specific and transcript-specific barcodes. The following cDNA amplification generated adequate quantities for library construction according to the standard protocol. Libraries were sequenced on an Illumina NovaSeq 6000 sequencing system (paired-end multiplexing run, 150 bp) by the LC-Bio Technology (Hangzhou, China) at a minimum depth of 20000 reads per cell.

scRNA-Seq data processing

We processed sequencing reads using CellRanger (version 6.0.1). Then we created objects by Seurat (version 4.0.5) R package, and merged data using the function of Merge[28]. The ratio of mitochondrial genes to all genetic material was used to judge whether a cell was in a steady state. Generally, it was thought that a cell might be in a state of stress when it had a higher proportion of mitochondrial genes. Therefore, we filtered cells with > 10% mitochondrial gene content. Considering potential cellular diploidy, we filtered cells with < 1000 or > 6000 genes. After the above steps, we finally obtained 17426 cells.

Data were normalized using the log-normalization method. After controlling for the relationship between mean expression and dispersion, we identified highly variable genes in individual cells. We input variable genes to perform principal component analysis (PCA) and identified significant principal components based on the function of JackStraw[29]. A total of 20 principal components were selected as statistically significant inputs to the Uniform Manifold Approximation and Projection (UMAP). We examined the distribution of UMAP and PCA between these samples. The data showed correlations. We compared the mean expression of genes between samples and found an excellent Pearson correlation between them. We divided the cells clustered by the FindCluster into 21 clusters.

Cell annotation

We identified cell types based on specific maker genes. The MSCs lineage was identified by *Col1a1* and *Col3a1*. *Lgals7* and *Krtdap* marked the epithelial cell lineage; muscle cell marker genes included *Actc1* and *Tnnt1*; macrophage marker genes included *Pf4* and *C1qb*; glial marker genes included *Dct* and *Ptgds*; T cell marker genes included *Cma1* and *Cpa3*; endothelial cell marker genes included *Egfl7* and *Cdh5*; and perivascular cell marker genes included *Rgs5* and *Ndufa4 L2*. The FindAllMarkers function was

used to find differentially expressed genes between each cell type.

Gene set enrichment analysis

Gene set enrichment analysis (GSEA) can identify whether predefined gene sets show significant differences between biological processes by a computational method. Typically, GSEA is used to estimate expression in dataset samples. To study differences in the biological processes between the two groups, we downloaded the reference gene set c2.cp.kegg.v7.4.entrez.gmt from the MSigDB database on the basis of the gene expression profiling dataset[30]. We used GSEA included in the R package Cluster-Profiler to perform enrichment analysis and visualization of the dataset. The cut-off standards were set as nominal $P < 0.05$, FDR q < 0.25 and normalized enrichment score (NES) > 0.6.

MSCs reclustering

On account of our main focus on MSCs, we extracted a subpopulation of MSCs. Based on hierarchical clustering and defined marker genes, we reclustered the MSCs using the FindClusters function and assigned the MSCs to 13 cell subpopulations. The progenitor subpopulation was identified by *Cdk1* and *Dkk1*, the osteoblasts subpopulation was identified by *Runx2* and *Sp7*, and the fibroblasts subpopulation was determined by maker genes *Dlk1* and *Shox2*. We next counted the proportions and number of these cell subpopulations in wild-type or *Cd271* knockout mice.

Gene ontology functional enrichment analysis and protein–protein interaction network

Gene Ontology (GO) is an approach for functional enrichment analysis of genes in diverse levels and dimensions. GO analysis comprises three levels: Biological process, molecular function and cellular components. The Wilcoxon rank-sum test was used to identify genes differentially expressed in MSCs between wild-type and *Cd271* knockout samples (logFC > 0.25, $P < 0.05$). Differentially expressed genes that were identified between wild-type and *Cd271* knockout samples were subjected to GO functional annotation by the ClusterProfiler (version 4.2.0) R package to identify the significantly enriched biological processes[31].The enrichment results were visualized in the form of a lollipop plot, and the significance threshold for the enrichment analysis was set at a corrected $P < 0.05$.

The STRING online database (https://string-db.org/) analyzed the interaction between the marker genes. We constructed a protein–protein interaction (PPI) network for the results obtained by Cytoscape (3.9.0). The functional interactions between the proteins expressed by the genes were mapped, including direct physical interactions and indirect functional correlations.

Pseudotemporal analysis

Cell differentiation of MSCs (progenitors, osteoblasts and fibroblasts) was inferred by the Monocle (2.22.0) R package and default parameters recommended by the developers[32]. The integrated gene expression profiling of each cell type was exported from Seurat into Monocle to establish the cellular gene dataset. The variable genes were defined by the process of DispersionTable, and the cells were sorted with the function of setOrderingFilter. The DDRTree method was used to reduce the dimension, and the orderCells function was used to estimate the cell arrangement along the trajectory. Based on clustering characteristics and marker gene analysis, we obtained the trajectory map of the differentiation time of MSCs. The study of each trajectory used a standard protocol with default parameters.

Cell–cell communication analysis

We identified the underlying interactions between MSCs and other cell populations by CellChat (version 1.1.3) (http://www.cellchat.org/) R package, which is commonly used to analyze cell–cell communication networks from single cell transcriptome sequencing profiling[33]. Taking advantage of CellChat, we inferred the scRNA-Seq data quantitatively and researched cell–cell communication networks. We predicted the main ingoing and outgoing signal patterns by network analysis and pattern recognition methods, as well as the coordination function between cells and signals. We counted all the important receptor–ligand pairs in the intercellular signal transmission by bubble chart, and we selected the signaling with a higher contribution to the cell for network centrality analysis.

Cell culture and mineralization induction

MSCs were isolated from embryonic maxillary processes. After washing with high-glucose Dulbecco's modified Eagle's medium (DMEM; Gibco, United States) three times, the cells were digested with trypsin–EDTA (Gibco) at 37 °C for 10 min, and centrifuged at 1000 rpm for 5 min. The cells were resuspended in a growth medium with DMEM, 10% fetal bovine serum (FBS) (Gibco), and 1% antibiotics (100 mg/mL penicillin and 100 µg/mL streptomycin) to generate primary MSCs. We maintained the cells at 37 °C in a 5% CO_2 humidified incubator and replaced the medium every 3 d.

For mineralization induction, cells were seeded in DMEM supplemented with 10% FBS at $4 × 10^4$ cells per well in 24-well plates. At 75%–80% confluence, we changed the medium to mineralization induction medium, which consisted of DMEM with 10% FBS, 100 IU/mL penicillin, 100 IU/mL streptomycin, 0.1 µM dexamethasone, 10 mmol/L β-glycerol phosphate (Sigma–Aldrich, St. Louis, MO, United States) and 50 µM ascorbic acid (Sigma–Aldrich). We cultured the cells for up to 7 d, and replaced the medium

every 3 d.

Alkaline phosphatase activity and staining

The alkaline phosphatase (ALP) activity kit (Nanjing Jiancheng Biotech, China) was used to detect intracellular ALP activity. Cells were lysed in RIPA lysis buffer (Beyotime, China) without protease and phosphatase inhibitors to induce mineralization for 7 d. We centrifuged the lysate at 12000 rpm and 4 °C for 30 min, and incubated the supernatant with reaction buffer at 37 °C for 15 min. We stopped the color development and measured the absorbance at 520 nm. We measured the protein concentration of the lysate with a Bicinchoninic Acid Assay (BCA) protein assay kit (Beyotime). The ALP staining assay was performed with a Beyotime kit. On day 7 of induction, the cells were fixed for 30 min and stained with Alkaline Phosphatase Assay Kit (Beyotime, China) in the dark for 30 min. The cells were observed and imaged for histochemical detection of ALP with a Nikon microscope.

Alizarin Red staining and quantification

After osteogenic inducting for 14 d, the cells were fixed with 4% paraformaldehyde for 30 min. They were stained with 1% Alizarin Red (pH 4.3) (Beyotime) for 20 min at room temperature and washed three times with deionized water. We observed and imaged the calcium deposits under a Nikon microscope. To quantify calcium deposits, we destained the stained cells with 10% cetylpyridinium chloride monohydrate (Sigma–Aldrich) in 10 mmol/L sodium phosphate (pH 7.0) for 30 min. We transferred a 200-μL aliquot to a 96-well plate to measure the absorbance at 550 nm by a Varioskan Flash Spectral Scanning Multimode Reader (ThermoFisher Scientific, United States).

Quantitative real-time polymerase chain reaction

Total RNA was isolated from the cells by an RNA prep pure Cell Kit (TIANGEN, Beijing, China). cDNA was synthesized following the instructions for the HiScript® III RT Super Mix for quantitative real time polymerase chain reaction (qPCR) kit (Vazyme, Nanjing, China). Quantitative real-time polymerase chain reaction (PCR) was performed with ChamQ Universal SYBR qPCR Master Mix kit (Vazyme) and Real-Time PCR Detection System (Quantstudio5, United States). Gene-specific primer pairs are show in Supplementary Table 1.

Cell Counting Kit-8 proliferation

Cell Counting Kit-8 (CCK-8; Dojindo Kagaku, Japan) was used to investigate the proliferation rate of E16.5d *Cd271* knockout and wild-type MSCs. The cells were seeded at 2×10^3 cells/well in a 96-well plate. After mixing the CCK-8 solution, the cells were cultured at 37 °C for 2 h in the dark. Absorbance was detected for 7 d continuously by a microplate reader at 450 nm.

Statistical analysis

Except the scRNA Seq, all the experiments were repeated more than three times. A one-way analysis of variance (ANOVA) or t test (GraphPad Prism 9.0 software, La Jolla, CA, United States) was used to identify significant differences. $P < 0.05$ was considered statistically significant.

RESULTS

scRNA-Seq analysis showed high cellular heterogeneity of murine maxillary process

To reveal cellular heterogeneity, we performed scRNA-Seq with murine maxillary processes from wild-type and *Cd271* knockout embryo tissues (Figure 1A and Supplementary Figure 1). After quality controlling and normalizing scRNA-Seq data, we obtained transcriptomes of 17426 cells (Supplementary Figure 2). UMAP clustering divided the cells into 21 independent clusters. Based on established lineage-specific marker genes, these 21 clusters were assigned to eight cell lineages (Figure 1B). We identified differentially expressed genes by comparing the gene expression profiles of one cluster with the others (Figure 1C). The MSC lineage was identified by *Col1a1* and *Col3a1*, and epithelial cells were marked by *Lgals7*. Based on these established lineage-specific maker genes, we assigned these clusters to eight cell types and plotted them (Figure 1D). We identified nine mesenchymal clusters (0–6, 11 and 17), a total of 12712 cells, which constituted the majority of sequenced cells by > 72.94%. Clusters 7, 18 and 20 were annotated as epithelial cells with a relative proportion of 6.14%. Muscle cells consisted of clusters 8, 9 and 12 with a relative proportion of 11.43%, while cluster 10 accounted for 3.11% as macrophages. Clusters 13 and 19 were annotated as glial cells (341, 1.95%). Clusters 14–16 were annotated as T cells (276, 1.58%), endothelial cells (269, 1.54%), and perivascular cells (162, 0.92%), respectively (Figure 1E).

We also analyzed the single cell sequence profiling from wild-type and *Cd271* knockout mice to establish the distribution of different types of cells and the source of samples. We counted the number and proportion of each cell type using histograms (Figure 1F). MSCs occupied most of the cell transcriptomes from the maxillary process, and the proportion of these cells between *Cd271* knockout
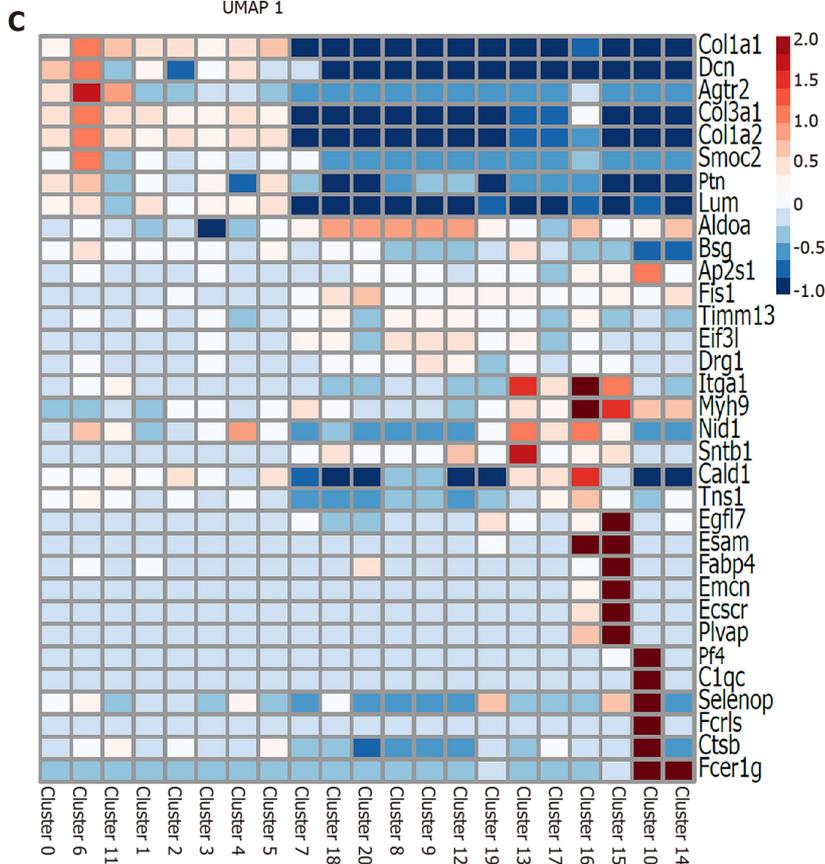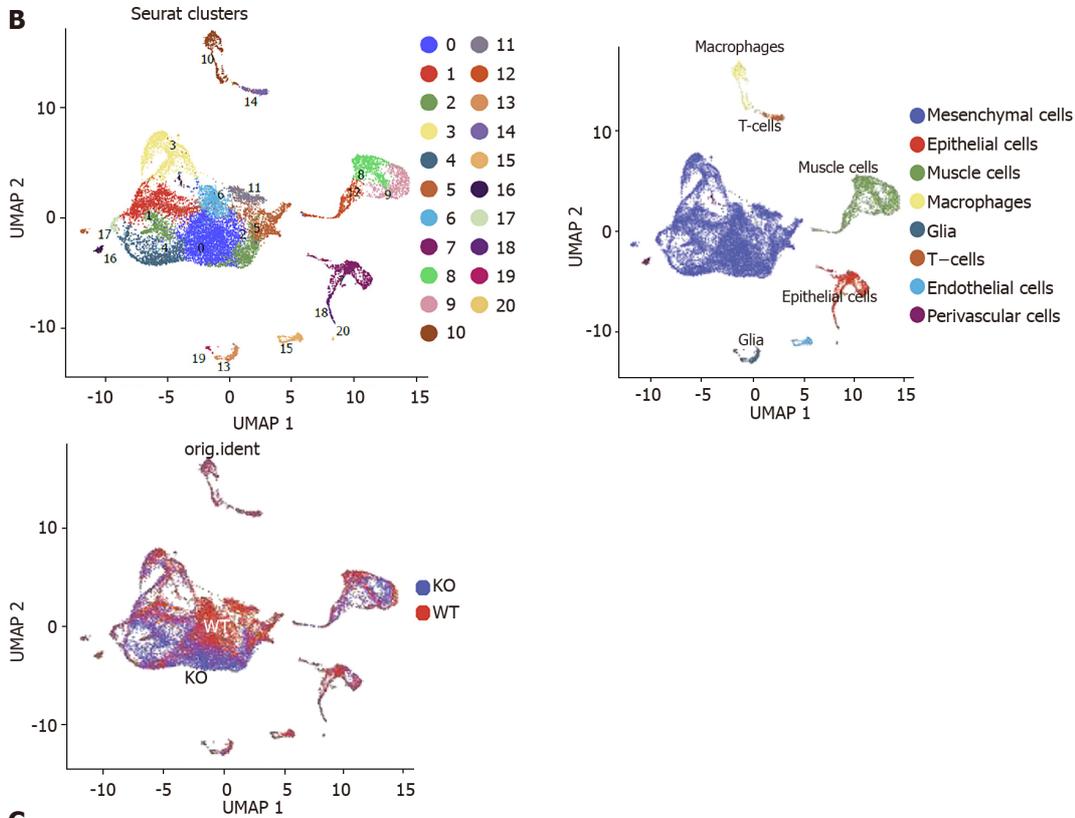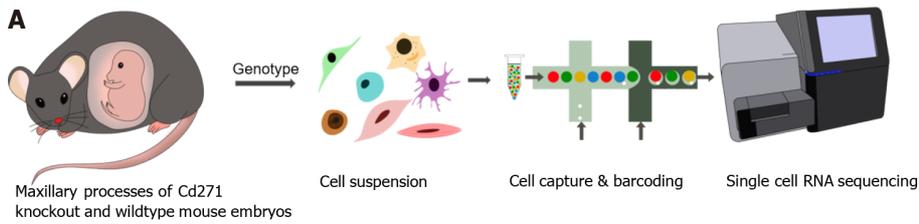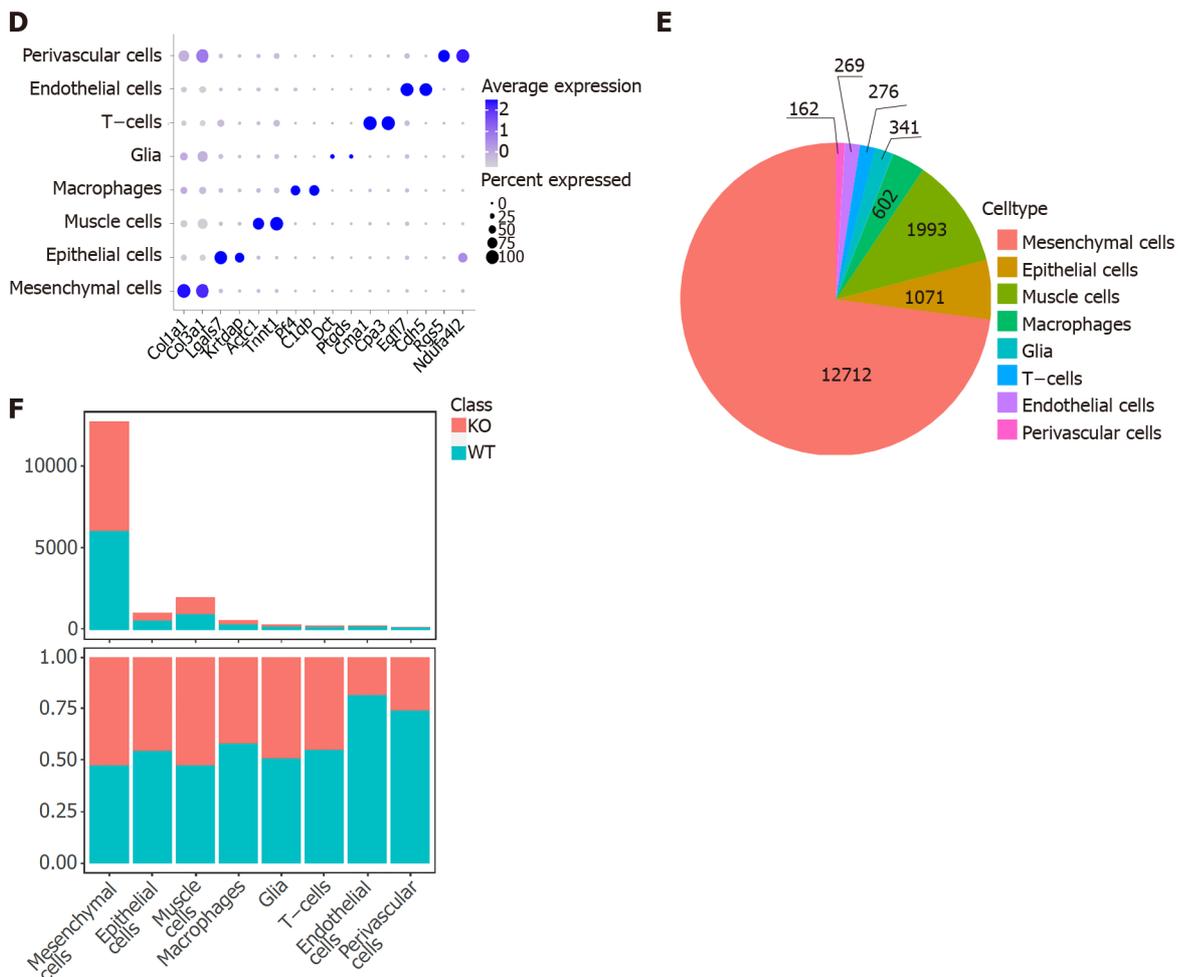
Figure 1 Single cell RNA sequencing analysis of maxillary processes from wild-type and *Cd271* knockout mice. We identified 21 clusters of cells, and the single cell RNA sequencing data were characterized. A: Schematic representation of the experimental workflow. The *Cd271* knockout and wild-type maxillary processes were collected from mouse embryos at 16.5 d. After genotyping, cells were suspended as single cells, and the cDNA library was constructed and sequenced; B: Cells extracted from the samples were subjected to Uniform Manifold Approximation and Projection hierarchical clustering and color-coded by cluster grouping, predominant cell type, and sample origin; C: Heatmap showing expression levels of differentially expressed genes in each cluster; D: Dot plot showing prominent marker genes for each cell type (mesenchymal cells, epithelial, muscle cell, macrophage, glial, T cell, endothelial, and perivascular); E: Pie chart showing the number of each cell type; F: Histogram showing the number and proportion of cells from wild-type and *Cd271* knockout mice. UMAP: Uniform Manifold Approximation and Projection; KO: Knockout; WT: Wild-type.

and wild-type was similar.

GSEA showed significant functional and signaling differences between cell types

To identify the relevant molecular mechanisms and possible pathways, we subjected all expressions to GSEA. The results showed a high correlation with MSCs and a close relationship with biomineralization. The results suggested that biomineralization (NES = 2.51, $P < 0.01$) and bone mineralization (NES = 2.49, $P < 0.001$) associated pathways enriched in MSCs (Figure 2A and B). GSEA also revealed that the differentially expressed genes enriched endothelial development, epithelial and glial cell differentiation, immune response, myofilament sliding and vascular smooth muscle contraction (Figure 2C–I).

Unsupervised clustering revealed novel subclusters of MSCs

As MSCs contribute much to embryogenesis and are essential in odontogenesis and osteogenesis, we performed unsupervised reclustering of MSCs. We performed the Subcluster analysis to investigate the heterogeneity within the mesenchymal populations. We observed further heterogeneity in subclusters 0–12 (Figure 3A). We used the published markers to identify the subclusters in MSCs. For instance, *Cdk1* and *Dkk1* marked progenitors, *Runx2* and *sp7* marked osteoblasts, and *Dlk1* and *Shox2* marked fibroblasts. We scored these marker genes in MSC clusters (Figure 3B). In this way, MSC clusters could also be identified into three subpopulations: Progenitors, fibroblasts and osteoblasts. We counted the cell proportions of the MSCs subclusters from wild-type and *Cd271* knockout maxillary processes. The
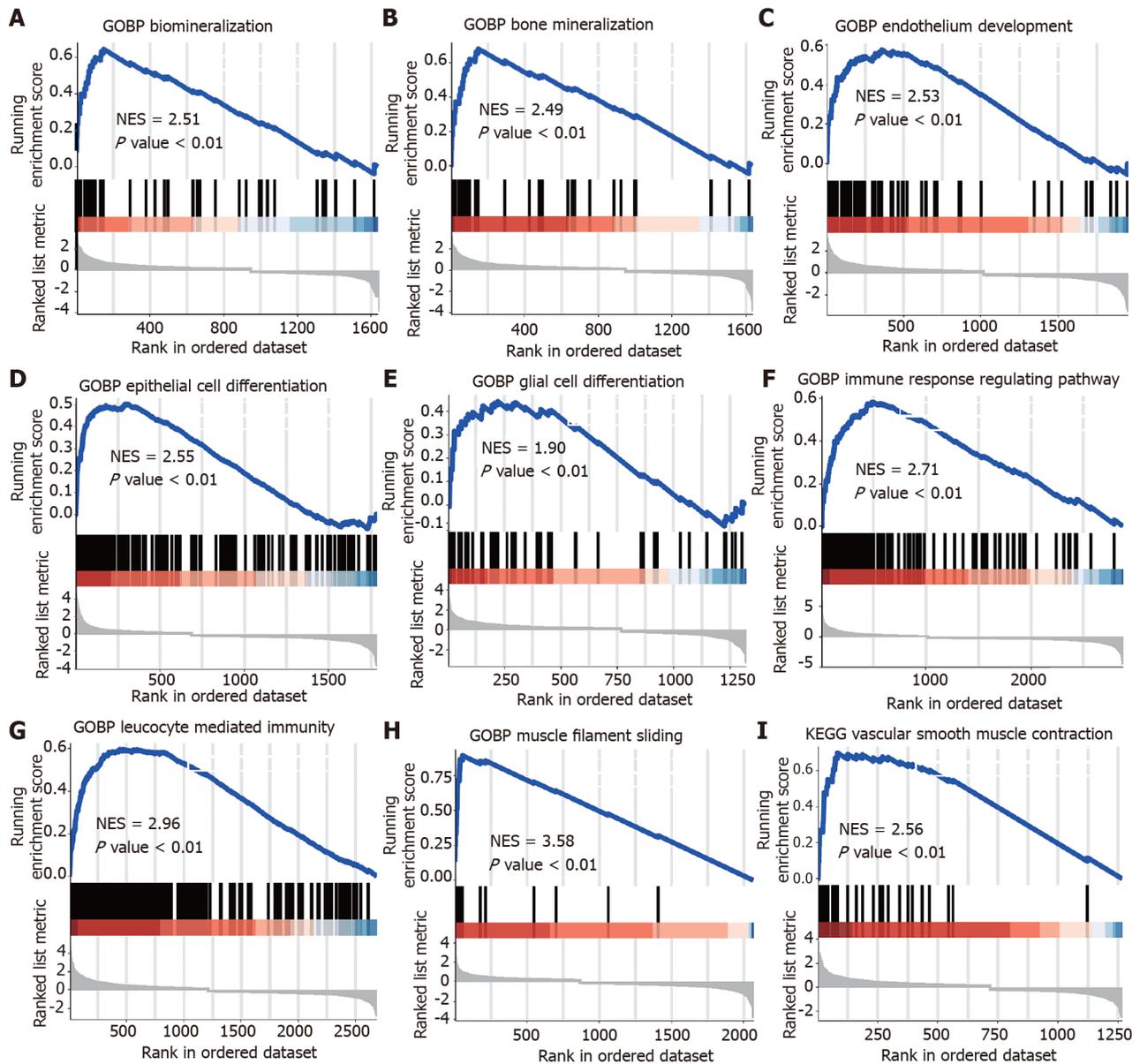
Figure 2 Gene set enrichment analysis plots for representative signaling pathways upregulated in maxillary process. Gene set enrichment analysis enriched differentially expressed genes into multifunctional gene networks. A and B: Representative gene set enrichment analysis maps for mesenchymal stem cells; C: Endothelial cells; D: Epithelial cells; E: Glia; F: T cells; G: Macrophages; H: Muscle cells; I: Perivascular cells. Normalized enrichment score normalized enrichment score, corrected for multiple comparisons using false discovery rate method, *P* values shown in plots. NES: Normalized enrichment score.

results showed that the numbers of subclusters 1, 3 and 10 were lower, while the other subclusters were higher in *Cd271* knockout compared with wild-type mice (Figure 3C).

Cd271 knockout MSCs exhibited weaker proliferation and osteogenic differentiation potential

We compared MSCs between wild-type and *Cd271* knockout maxillary processes. GO functional enrichment analysis revealed that differentially expressed genes were enriched in ossification, myeloid cell differentiation and biomineralization cell proliferation-related signaling (Figure 4A). To compare the differences in proliferation and osteogenic differentiation between wild-type and *Cd271* knockout MSCs, we investigated the potential for MSC proliferation. As the CCK-8 assay showed, the *Cd271* knockout MSCs exhibited weaker cell proliferation (Figure 4B). We induced the cells with an osteogenic induction medium and performed the mineralization assay. ALP staining and a quantitative assay revealed a lower and lighter mineralization level of *Cd271* knockout than wild-type MSCs. Lighter and fewer mineralized nodules were observed by Alizarin Red staining in *Cd271* knock out MSCs (Figure 4C). These results indicated more inadequate osteogenic differentiation potential in *Cd271* knockout MSCs. We selected several differentially expressed genes with considerable interaction by
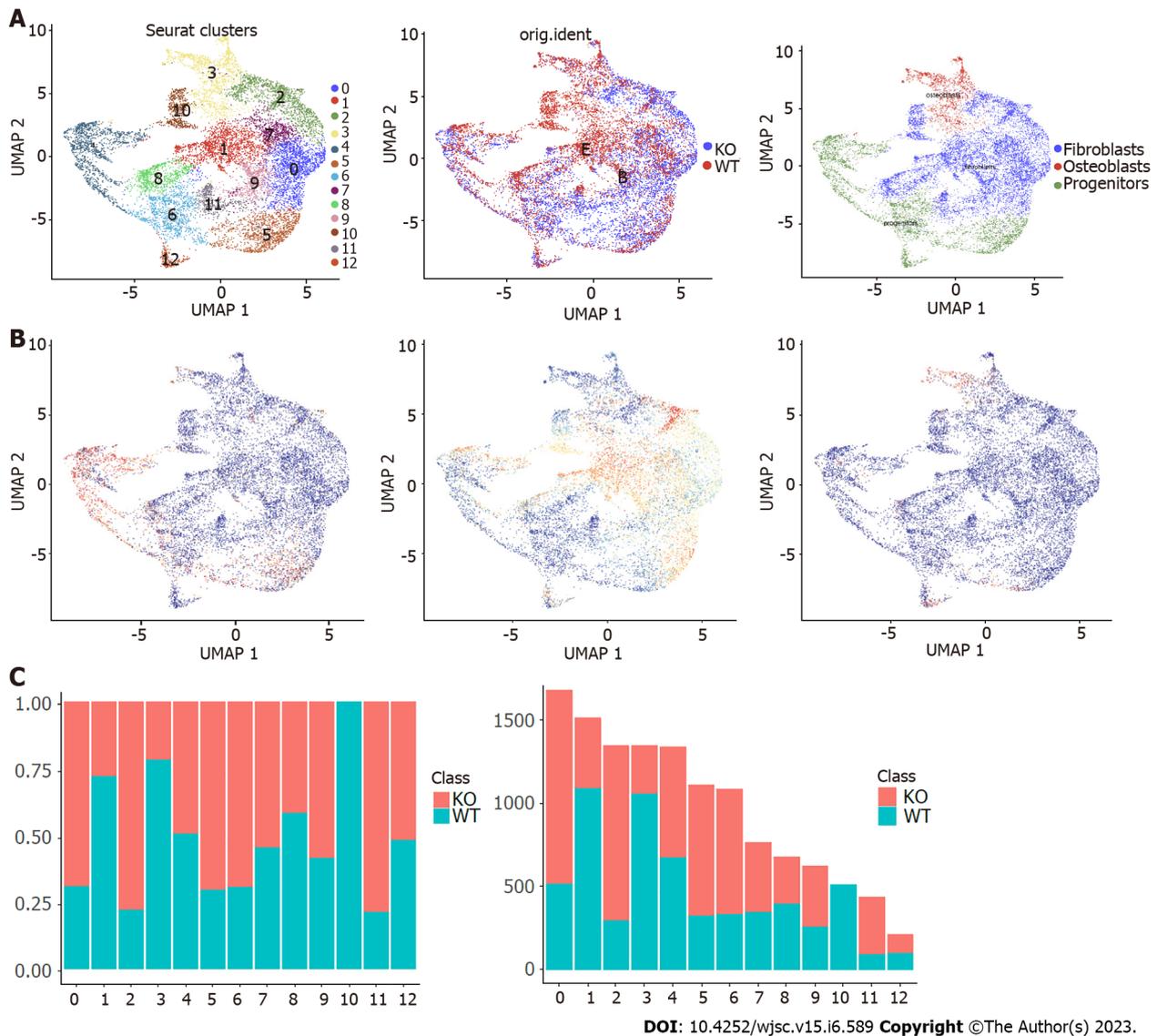
Figure 3 Further cluster analysis of mesenchymal stem cells. A: Mesenchymal stem cells were reclustered and color-coded according to cluster, sample origin and cell type; B: Feature scores of progenitors, fibroblasts and osteoblasts marker genes were displayed in the Uniform Manifold Approximation and Projection plot; C: Histogram showing the proportion and the number of cells in each cluster of wild-type and *Cd271* knockout mice. UMAP: Uniform Manifold Approximation and Projection; KO: Knockout; WT: Wild-type.

Cytoscape, and measured the gene expression by real-time quantitative PCR (Figure 4D). Proliferation, ossification and osteoblast differentiation-related genes, such as *Col4a1*, *Col6a1*, *Sparc*, *Vim*, *Col1a1* and *Col3a1*, were significantly decreased in *Cd271* knockout MSCs (Figure 4E). *Cd271* was involved in regulating osteogenic differentiation in MSCs, and our results implied a weaker potential of proliferation and osteogenic differentiation in *Cd271* knockout MSCs.

Different sets of genes appeared to shift along the differentiation trajectory

We selected MSCs to institute a pseudotemporal trajectory map that contained terminals consistent with distinct cell fates. The progenitor cells aggregated at the root and branches, indicating a good cell cycle of the progenitor cells. Osteoblasts and fibroblasts were scattered in various branches, showing high invasive potential (Figure 5A–C). We extracted differentially expressed genes over pseudotemporal changes and plotted heatmaps. Different sets of genes were also found to be shifted during the progression of MSCs, stressing the actional change of the progenitor cells, which managed the cell fate transition in the mesenchyme. We clustered the differentially expressed genes into three and performed GO analysis. Clusters 1 and 2 were significantly enriched in biological processes of osteoblast differentiation, biomineralization and odontogenesis, while cluster 3 was mainly enriched in cell metabolism (Figure 5D).

Cell–cell interactions of mesenchymal subpopulations were crucial in the maxillary process

The dataset of scRNA-Seq provided an opportunity to analyze intercellular communication mediated by
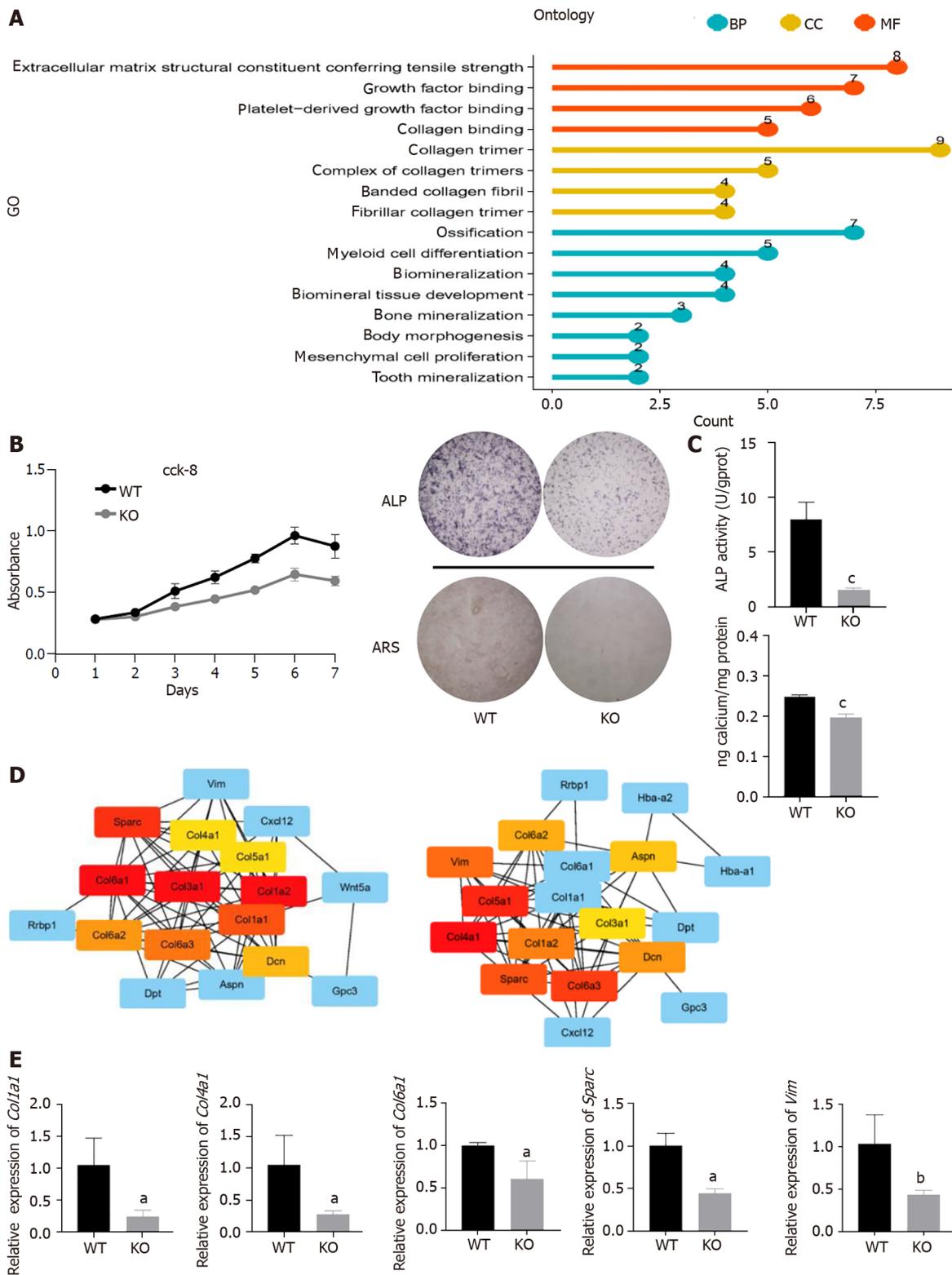
DOI: 10.4252/wjsc.v15.i6.589 **Copyright** ©The Author(s) 2023.

Figure 4 *Cd271* knockout mesenchymal stem cells showed weaker proliferation and osteogenic differentiation potential. A: Gene Ontology enrichment analysis of differentially expressed genes between *Cd271* knockout and wild-type mesenchymal stem cells (MSCs); B: Growth curves of *Cd271* knockout and wild-type MSCs; C: Mineralization assay of *Cd271* knockout and wild-type MSCs. Alkaline phosphatase (ALP) and Alizarin red staining of *Cd271* knockout MSCs was significantly lighter. ALP activity and calcium quantification were significantly lower in *Cd271* knockout compared with wild-type MSCs; D: Protein–protein interaction network interaction analysis of wildtype *vs Cd271* knockout differentially expressed genes; E: Quantitative real-time polymerase chain reaction assay of some differentially expressed genes in *Cd271* knockout and wild-type MSCs. Data are presented as mean values ± SD (*n* = 3 biologically independent experiments. Two-sided unpaired t-test, [a]*P* < 0.05, [b]*P* < 0.01, [c]*P* < 0.001) BP: Biological Process; CC: Cell component; MF: Molecular function; ARS: Alizarin red S; ALP: Alkaline phosphatase; KO: Knockout; WT: Wild-type.
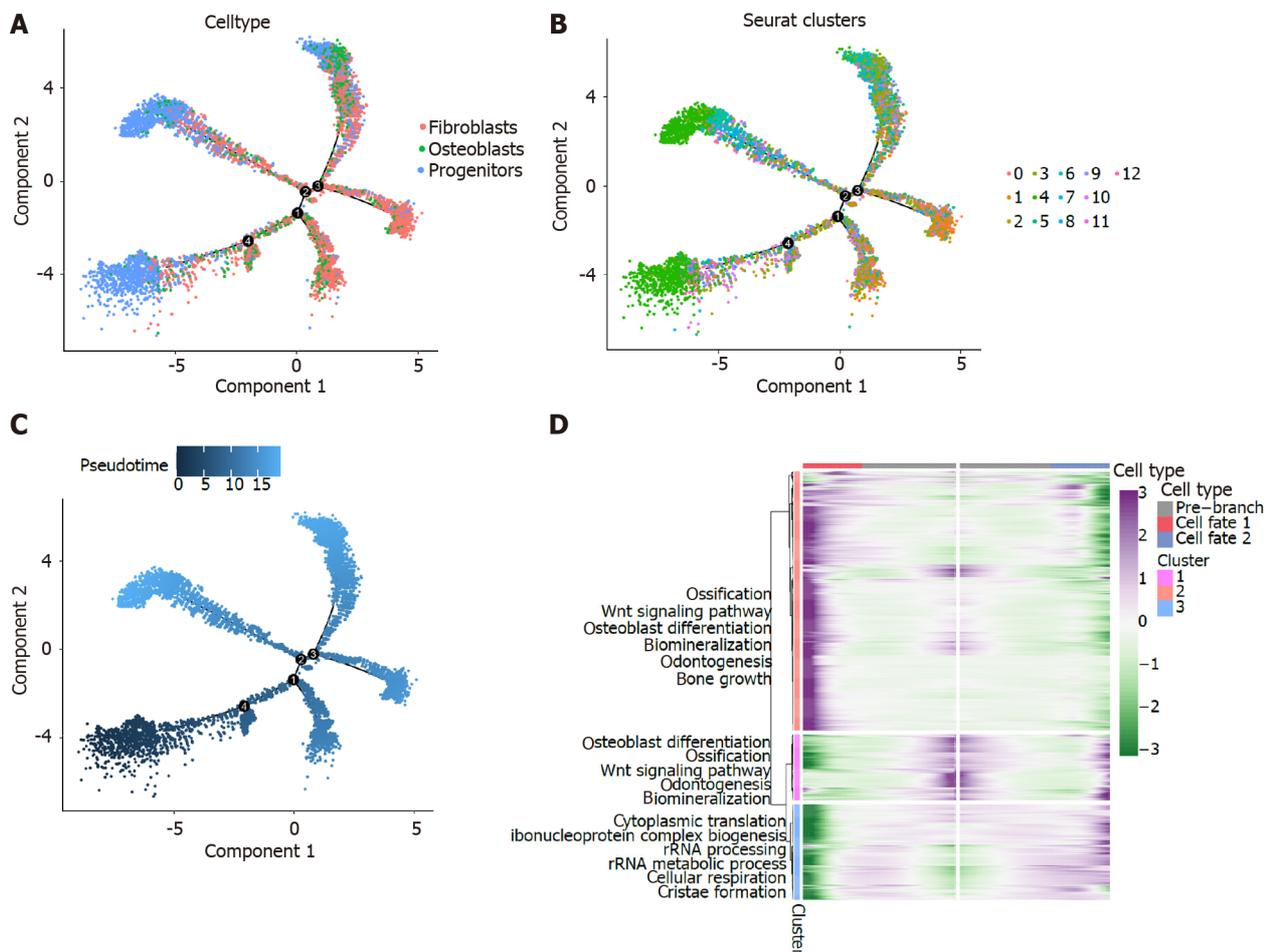
**DOI**: 10.4252/wjsc.v15.i6.589 **Copyright** ©The Author(s) 2023.

Figure 5 The potential developmental trajectories of mesenchymal stem cells by Monocle. A: Pseudo-sequential diagram based on the differentiation process of mesenchymal stem cell (MSC) subpopulations; B: Pseudo-sequence plot of MSCs colored by cluster classification; C: Pseudo-sequential diagram of MSCs drawn with timeline coloring; D: Heatmap of differentially expressed genes in pseudotemporal analysis. The differentially expressed genes were divided into three gene clusters and gene ontology biological process enrichment analysis was performed.

ligand–receptor interactions. To gain insights into potential signaling interactions between different cellular subpopulations, we interrogated our data with CellChat (version 1.1.3) (http://www.cellchat.org/) R package, which could predict the ligand and receptor interactions at single cell resolution[33]. We found dense communication between MSCs and other cells, and the most concentrated interactions occurred in the mesenchymal subpopulation (Figure 6A and B). It revealed the importance of mesenchymal interaction signaling. We detected 30 signaling pathways in eight cell groups, including MK, PTN, ncWNT, IGF, PDGF, WNT and VEGF signaling pathways. We compared the contribution of efferent (or afferent) signaling between cells, confirming that MSCs had higher interaction than other cell types while acting as outgoing signaling pathways (Figure 6C). We analyzed the potential signaling of MSCs, revealing a series of signaling pathways, such as odontogenesis-related signaling such as WNT, BMP and HH signaling (Figure 6D).

We explored ligand–receptor signals broadcast by MSCs, which revealed that MSCs might affect other cells in the ligand–receptor interaction of MK and PTN signaling (Figure 6E). We performed network centrality analysis on MK and PTN signaling, which confirmed that MSCs were important signal senders in intercellular communication (Figure 6F and G). The expression of *Mdk* and *Ptn* in wild-type and *Cd271*$^{-/-}$ MSCs exhibited significant differences by quantitative real-time PCR assay. The expression of *Mdk* and *Ptn* was higher in the *Cd271* knockout MSCs (Figure 6H). These results disclosed underlying ligand–receptor interactions and suggested that MK and PTN signaling may be influenced by *Cd271* in mesenchymal subpopulations.

DISCUSSION

Although MSCs have been extensively studied, there is still a lack of knowledge about the key
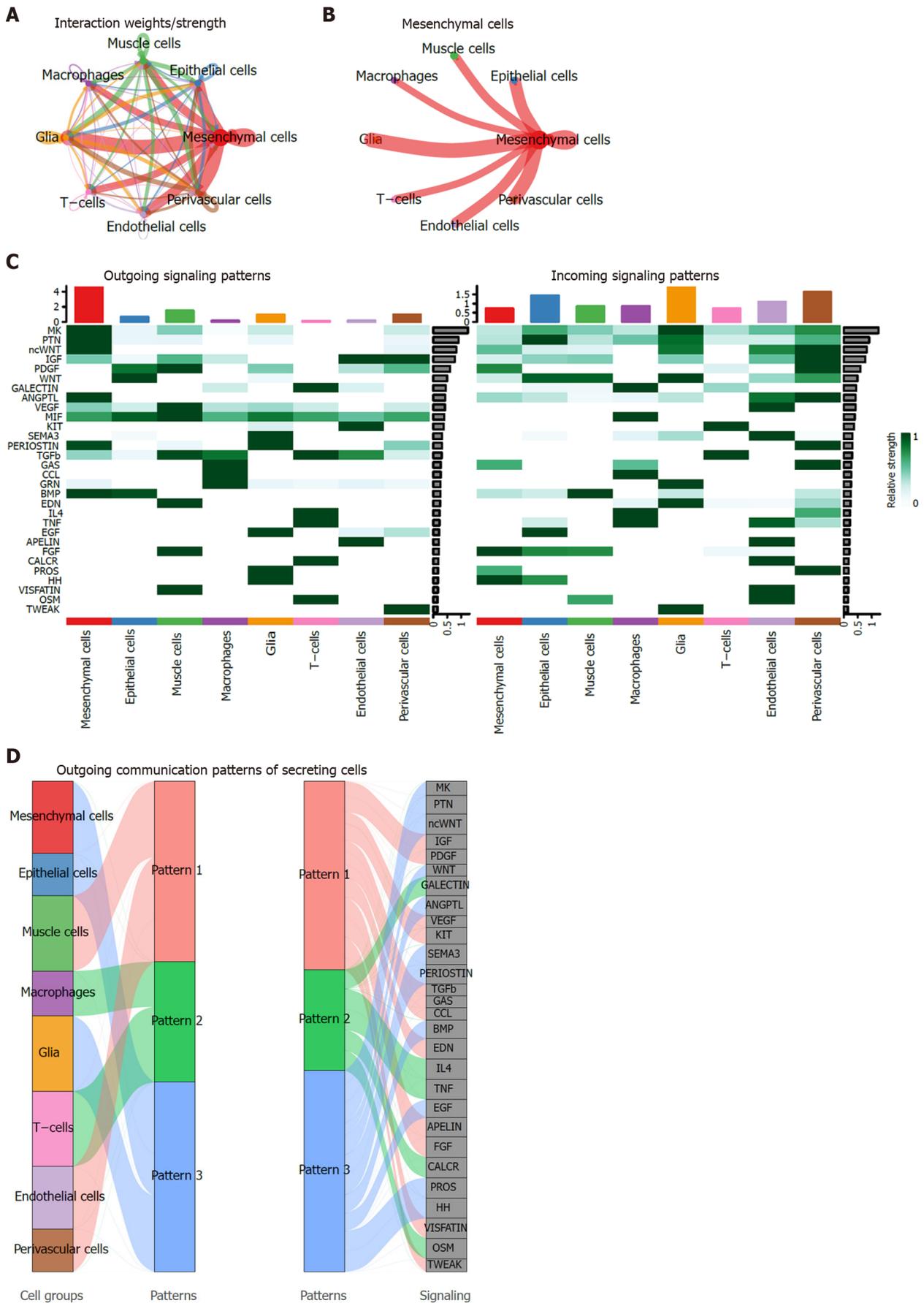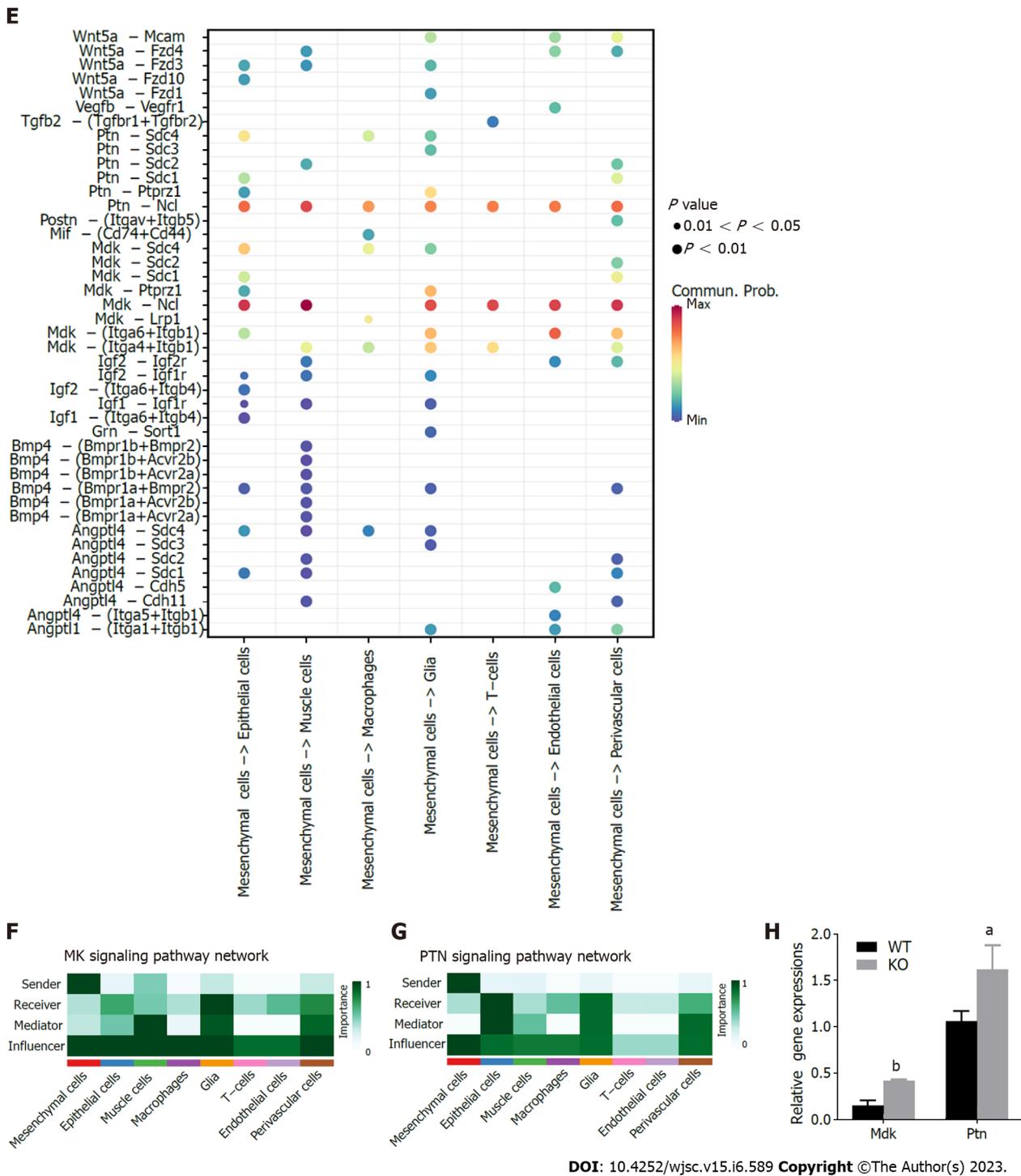
Figure 6 Inference, analysis and visualization of cellular communication networks from a single dataset *via* CellChat. A: Interaction intensity plot between cells in single cell sequence profiling; B: Interaction intensity map between mesenchymal stem cells (MSCs) and other cell types; C: Contribution map of 30 signaling pathways detected by CellChat to intercellular efferent (or afferent) signaling; D: Alluvial plot of cell outgoing signaling patterns, showing the correspondence between cell populations and signaling pathways; E: Important ligand–receptor pairs for MSCs sending signals to other cell types. F and G: Contribution of efferent (or afferent) signals between cells, the MK signaling pathway (F) and PTN signaling pathway (G) were selected for visualization of network centrality scores; H: Expression of *Mdk* and *Ptn* in *Cd271* knockout and wild-type MSCs was analyzed by quantitative real-time polymerase chain reaction. Data are presented as mean values ± SD (*n* = 3 biologically independent experiments. Two-sided unpaired *t*-test, [a]*P* < 0.05, [b]*P* < 0.01). KO: Knockout; WT: Wild-type.

mechanisms in tooth development. Researchers have found that the maxillary process included various cell subpopulations with diverse phenotypic and functional characteristics[34]. How this heterogeneity appears in osteogenesis and odontogenesis remains unclear. *Cd271* used to be a marker of the MSCs, and it had been reported that *Cd271* promotes differentiation in MSCs[35-37]. Hence, we used *Cd271* knockout mouse embryos to investigate what happens to MSCs in their initial developmental stage. We constructed a single cell profiling of representative mouse embryo maxillary processes and selected MSCs to explore their characteristics and critical regulatory mechanism *Cd271* related.

Maxillary-process-derived MSCs are recognized as primitive odontogenic stem cells. For instance, researchers obtained the MSCs from the first branchial arch of mice and the maxillary process tissue of rats in succession, and revealed the pluripotency of MSCs[38,39]. Wen *et al*[40] found that p75^{+/+} MSCs have good multidirectional differentiation potential[40]. We identified nine MSC clusters among 21 clusters identified using scRNA-Seq in mouse embryo maxillary processes. MSC clusters accounted for the majority, suggesting that MSCs contribute much to embryogenesis. Emerging studies have revealed that the marker genes of MSCs, *Col1a1* and *Col3a1*, promote collagen production and influence odontogenesis or osteogenesis[41-43]. The decreased expression of these two genes in *Cd271* knockout MSCs compared to wild-type, suggested that *Cd271* was related to MSC regulation of odontogenesis or osteogenesis.

In the past, several studies concentrated on the whole population of MSCs rather than the relationships among the subclusters. Our subcluster analysis disclosed that these MSC clusters could be separated into three subpopulations: Fibroblast, progenitors and osteoblast, which had not been separated before. One of the characteristics of MSC clusters is the expression of osteoblast differentiation-associated genes such as *Runx2*, *Sox9*, *Msx1* and *Omd*[44-47]. Previous studies showed that proteins such as Runx2 and Sox9 were positively regulated by *Cd271* in MSCs[48-50]. However, these studies did not show the heterogeneity of MSCs, or which subpopulations of MSCs these proteins derived from. Our results revealed that these proteins were mainly expressed in the osteoblast subpopulation. The number of osteoblast subpopulations decreased while progenitor subpopulations increased. This suggested that some progenitors were hindered from differentiating into osteoblasts in the *Cd271* knockout MSC clusters. Consistently, GO enrichment analysis and GSEA verified significant enrichment of the ossification, biomineralization and bone mineralization pathways in the *Cd271* knockout and wild-type cells. Based on our scRNA-Seq data, we gained differentially expressed genes between two groups for the first time. We picked out several differentially expressed genes with extensive interactions; for instance, *Sparc*, *Vim*, *Col4a1*, *Col6a1*, *Col1a1* and *Col3a1*. These genes are considered to relate to cell proliferation, bone mineralization and multipotent differentiation[41-43,51-54]. In *Cd271* knockout MSCs, we verified by quantitative real-time PCR that these differentially expressed gene clusters had lower expression. Functional experiments also demonstrated a weaker odontogenic and osteogenic differentiation and proliferation in the *Cd271* knockout MSCs. Consistent with previous studies, our results confirmed that the MSC clusters had an essential role in odontogenesis and osteogenesis and *Cd271* possibly regulated it.

Pseudotemporal analysis uncovered a developmental trajectory among these three subpopulations. Significantly, the progenitor subpopulation was found to develop into the osteoblast and fibroblast subpopulations. We concluded that the progenitors were the base subpopulation and increasingly transformed into the osteoblast and fibroblast subpopulations in MSCs. Consistent with our GO and GSEA findings, the differentially expressed genes that emerged in pseudotemporal analysis showed a significant relation with ossification and osteoblast differentiation in MSCs. Collectively, our results revealed that MSCs were progressively diversified and determined to the odontogenic fate. Thus, the mesenchyme in the maxillary process provides a remarkable model to study the development of maxillary-process-derived MSCs.

It is known that the interactions between dental mesenchyme and epithelium play a crucial part in the integral tooth developmental process. Nevertheless, the cell–cell interactions within the maxillary process have not been extensively studied[55]. In our study, scRNA-Seq offered the opportunity to identify communicating pairs on the basis of the expression of their cell-surface receptors and ligands. CellChat showed that the most concentrated interactions occurred between mesenchymal and other cells. It indicated that MSCs play a vital role in cell communication. It is worth noting that MSCs mainly participated in MK, PTN, ncWNT, WNT and BMP signaling. Previous studies reported that *Cd271* might regulate the odontogenic differentiation of MSCs through the BMP, WNT and PI3K pathways[17, 49,56]. However, there are no reports that MDK signaling participates in regulating MSCs. In the CellChat, the receptor interactions of MDK and PTN appeared to be obvious. It reminded us that the *Mdk* and *Ptn* might play a primary role in the developmental process of MSCs. *Mdk* and *Ptn* expression notably increased in *Cd271* knockout cells during induction of mineralization for 7 d. Our subsequent study will explore the molecular mechanism of how *Cd271* regulates *Mdk* to influence osteogenesis.

Although our studies revealed several significant discoveries, there were some limitations. First, different clustering can generate different results; thus, further groupings are needed to perform future analysis. Second, the current study was based on scRNA-Seq. Therefore, we did some biological observation but did not illustrate the direct mechanisms of *Cd271* involved in tooth development. Therefore, further studies about direct mechanisms and *in vivo* studies are needed.

CONCLUSION

Our study reveals high cellular heterogeneity, molecular details and cell-cell interactions in MSCs. It provides a valuable resource for understanding the development of maxillary-process-derived MSCs. And it enables the maxillary process to serve as an excellent model to explore tooth development and

cell fate determinations. Furthermore, we have found significant functional and signaling differences between *Cd271* knockout and wildtype MSCs. We have clarified that *Cd271* is significantly associated with the regulation of mineralization. We tentatively propose that *Mdk* signaling is involved in the regulatory mechanism of mineralization. These findings contribute to thorough exploration of the mechanism of *Cd271* in regulating odontogenesis and osteogenesis which add to the theory of tooth development.

ARTICLE HIGHLIGHTS

Research background

Tooth loss has become a common problem in human life. Compared with traditional denture restoration, dental tissue engineering has become the most ideal means to solve this problem, and it is also one of the most active research fields of stomatology in recent years. The tooth development involves complex signal pathways. Ecto-mesenchymal stem cells (MSCs) were regarded as the primitive dental cells in the classical theory of tooth development. To date, in-depth studies of the odontogenesis and osteogenesis of MSCs are still lacking.

Research motivation

We contribute to thorough exploration of the mechanism of odontogenesis and osteogenesis to add to the theory of tooth development.

Research objectives

Our study provides novel insights into the biological features of MSCs at the single cell level and the mechanism of *Cd271* in regulating odontogenesis and osteogenesis.

Research methods

We used the maxillary process from mouse embryos as a model to understand the development of maxillary-process-derived MSCs. We applied single cell RNA sequence analysis to elucidate the cellular heterogeneity and explore molecular details. And we verified the findings from single cell sequencing *in vitro* by lab experience such as cell staining, cell counting and quantitative real time polymerase chain reaction.

Research results

Our study reveals: (1) High cellular heterogeneity and molecular details; (2) Significant functional and signaling differences between cell types; (3) Novel subclusters of mesenchymal stem cells; and (4) Crucial cell-cell interactions of mesenchymal subpopulations. Besides, we contribute to thorough exploration of the mechanism of *Cd271* in regulating odontogenesis and osteogenesis.

Research conclusions

Our study reveals high cellular heterogeneity, molecular details and cell-cell interactions in MSCs. We found significant functional and signaling differences between *Cd271* knockout and wildtype MSCs. We clarified that *Cd271* is significantly associated with the regulation of mineralization.

Research perspectives

We need illustrate that *Mdk* signaling is involved in the regulatory mechanism of mineralization in future research. And direct mechanisms of *Cd271* involved in tooth development are needed in further studies.

FOOTNOTES

Institutional animal care and use committee statement: All animal experiments were performed according to the protocols approved by the Medical Ethics Committee of Wenzhou Medical University, No. wydw2019-0224.

ORCID number: Yan-Yan Zhang 0000-0001-6233-5752; Feng Li 0000-0002-0172-388X; Xiao-Ke Zeng 0000-0003-1643-1932; Yan-Hui Zou 0000-0002-6543-3796; Bing-Bing Zhu 0000-0001-8306-6109; Jia-Jia Ye 0000-0001-5901-3453; Yun-Xiao Zhang 0000-0002-0799-2642; Qiu Jin 0000-0003-3830-2613; Xin Nie 0000-0002-4645-226X.

REFERENCES

1   **Egbuniwe O**, Idowu BD, Funes JM, Grant AD, Renton T, Di Silvio L. P16/p53 expression and telomerase activity in immortalized human dental pulp cells. *Cell Cycle* 2011; **10**: 3912-3919 [PMID: 22067611 DOI: 10.4161/cc.10.22.18093]

2   **Strobl-Mazzulla PH**, Bronner ME. Epithelial to mesenchymal transition: new and old insights from the classical neural crest model. *Semin Cancer Biol* 2012; **22**: 411-416 [PMID: 22575214 DOI: 10.1016/j.semcancer.2012.04.008]

3   **Abbasian M**, Langlois A, Gibon J. Sexual Dimorphism in Balance and Coordination in p75NTR(exonIII) Knock-Out Mice. *Front Behav Neurosci* 2022; **16**: 842552 [PMID: 35283743 DOI: 10.3389/fnbeh.2022.842552]

4   **Alvarez R**, Lee HL, Hong C, Wang CY. Single CD271 marker isolates mesenchymal stem cells from human dental pulp. *Int J Oral Sci* 2015; **7**: 205-212 [PMID: 26674422 DOI: 10.1038/ijos.2015.29]

5   **Akiyama Y**, Mikami Y, Watanabe E, Watanabe N, Toriumi T, Takahashi T, Komiyama K, Isokawa K, Shimizu N, Honda MJ. The P75 neurotrophin receptor regulates proliferation of the human MG63 osteoblast cell line. *Differentiation* 2014; **87**: 111-118 [PMID: 24582280 DOI: 10.1016/j.diff.2014.01.002]

6   **Castellini C**, Mattioli S, Cotozzolo E, Pistilli A, Rende M, Bartolini D, Di Sante G, Menchetti L, Dal Bosco A, Stabile AM. The Effect of Interaction NGF/p75(NTR) in Sperm Cells: A Rabbit Model. *Cells* 2022; **11** [PMID: 35326486 DOI: 10.3390/cells11061035]

7   **Zanin JP**, Friedman WJ. p75NTR prevents the onset of cerebellar granule cell migration *via* RhoA activation. *Elife* 2022; **11** [PMID: 36040414 DOI: 10.7554/eLife.79934]

8   **Zhao H**, Fan S, Sun J. Delayed wound healing in the elderly and a new therapeutic target: CD271. *Curr Stem Cell Res Ther* 2023 [PMID: 37016526 DOI: 10.2174/1574888X18666230403083603]

9   **Passino MA**, Adams RA, Sikorski SL, Akassoglou K. Regulation of hepatic stellate cell differentiation by the neurotrophin receptor p75NTR. *Science* 2007; **315**: 1853-1856 [PMID: 17395831 DOI: 10.1126/science.1137603]

10   **Wen X**, Liu L, Deng M, Liu R, Zhang L, Nie X. In vitro cementoblast-like differentiation of postmigratory neural crest-derived p75(+) stem cells with dental follicle cell conditioned medium. *Exp Cell Res* 2015; **337**: 76-86 [PMID: 26165934 DOI: 10.1016/j.yexcr.2015.07.001]

11   **Baeza-Raja B**, Sachs BD, Li P, Christian F, Vagena E, Davalos D, Le Moan N, Ryu JK, Sikorski SL, Chan JP, Scadeng M, Taylor SS, Houslay MD, Baillie GS, Saltiel AR, Olefsky JM, Akassoglou K. p75 Neurotrophin Receptor Regulates Energy Balance in Obesity. *Cell Rep* 2016; **14**: 255-268 [PMID: 26748707 DOI: 10.1016/j.celrep.2015.12.028]

12   **Gonçalves NP**, Mohseni S, El Soury M, Ulrichsen M, Richner M, Xiao J, Wood RJ, Andersen OM, Coulson EJ, Raimondo S, Murray SS, Vægter CB. Peripheral Nerve Regeneration Is Independent From Schwann Cell p75(NTR) Expression. *Front Cell Neurosci* 2019; **13**: 235 [PMID: 31191256 DOI: 10.3389/fncel.2019.00235]

13   **Smith RJP**, Faroni A, Barrow JR, Soul J, Reid AJ. The angiogenic potential of CD271+ human adipose tissue-derived mesenchymal stem cells. *Stem Cell Res Ther* 2021; **12**: 160 [PMID: 33653407 DOI: 10.1186/s13287-021-02177-0]

14   **Mitsiadis TA**, Pagella P. Expression of Nerve Growth Factor (NGF), TrkA, and p75(NTR) in Developing Human Fetal Teeth. *Front Physiol* 2016; **7**: 338 [PMID: 27536251 DOI: 10.3389/fphys.2016.00338]

15   **Zhao X**, Ning L, Xie Z, Jie Z, Li X, Wan X, Sun X, Huang B, Tang P, Shen S, Qin A, Ma Y, Song L, Fan S, Wan S. The Novel p38 Inhibitor, Pamapimod, Inhibits Osteoclastogenesis and Counteracts Estrogen-Dependent Bone Loss in Mice. *J Bone Miner Res* 2019; **34**: 911-922 [PMID: 30615802 DOI: 10.1002/jbmr.3655]

16   **Colosimo A**, Rofani C, Ciraci E, Salerno A, Oliviero M, Maio ED, Iannace S, Netti PA, Velardi F, Berardi AC. Osteogenic differentiation of CD271(+) cells from rabbit bone marrow cultured on three phase PCL/TZ-HA bioactive scaffolds: comparative study with mesenchymal stem cells (MSCs). *Int J Clin Exp Med* 2015; **8**: 13154-13162 [PMID: 26550238]

17   **Xing Y**, Nie X, Chen G, Wen X, Li G, Zhou X, Tian W, Liu L. Comparison of P75 NTR-positive and -negative

etcomesenchymal stem cell odontogenic differentiation through epithelial-mesenchymal interaction. *Cell Prolif* 2016; **49**: 185-194 [PMID: 27038014 DOI: 10.1111/cpr.12248]

18   **Li Z**, Zhang C, Weiner LP, Zhang Y, Zhong JF. Molecular characterization of heterogeneous mesenchymal stem cells with single-cell transcriptomes. *Biotechnol Adv* 2013; **31**: 312-317 [PMID: 23266308 DOI: 10.1016/j.biotechadv.2012.12.003]

19   **Chen Y**, Zhang Z, Yang X, Liu A, Liu S, Feng J, Xuan K. Odontogenic MSC Heterogeneity: Challenges and Opportunities for Regenerative Medicine. *Front Physiol* 2022; **13**: 827470 [PMID: 35514352 DOI: 10.3389/fphys.2022.827470]

20   **Tanay A**, Regev A. Scaling single-cell genomics from phenomenology to mechanism. *Nature* 2017; **541**: 331-338 [PMID: 28102262 DOI: 10.1038/nature21350]

21   **Yan H**, Ye Y, Zhao H, Zuo H, Li Y. Single-Cell RNA Sequencing for Analyzing the Intestinal Tract in Healthy and Diseased Individuals. *Front Cell Dev Biol* 2022; **10**: 915654 [PMID: 35874838 DOI: 10.3389/fcell.2022.915654]

22   **Li Y**, Ju S, Li X, Li W, Zhou S, Wang G, Cai Y, Dong Z. Characterization of the microenvironment of diabetic foot ulcers and potential drug identification based on scRNA-seq. *Front Endocrinol (Lausanne)* 2022; **13**: 997880 [PMID: 36686438 DOI: 10.3389/fendo.2022.997880]

23   **Liu X**, Xiang Q, Xu F, Huang J, Yu N, Zhang Q, Long X, Zhou Z. Single-cell RNA-seq of cultured human adipose-derived mesenchymal stem cells. *Sci Data* 2019; **6**: 190031 [PMID: 30806636 DOI: 10.1038/sdata.2019.31]

24   **Kirkwood PM**, Gibson DA, Smith JR, Wilson-Kanamori JR, Kelepouri O, Esnal-Zufiaurre A, Dobie R, Henderson NC, Saunders PTK. Single-cell RNA sequencing redefines the mesenchymal cell landscape of mouse endometrium. *FASEB J* 2021; **35**: e21285 [PMID: 33710643 DOI: 10.1096/fj.202002123R]

25   **Wang Z**, Li X, Yang J, Gong Y, Zhang H, Qiu X, Liu Y, Zhou C, Chen Y, Greenbaum J, Cheng L, Hu Y, Xie J, Yang X, Li Y, Schiller MR, Tan L, Tang SY, Shen H, Xiao HM, Deng HW. Single-cell RNA sequencing deconvolutes the in vivo heterogeneity of human bone marrow-derived mesenchymal stem cells. *Int J Biol Sci* 2021; **17**: 4192-4206 [PMID: 34803492 DOI: 10.7150/ijbs.61950]

26   **Bayarsaihan D**, Enkhmandakh B, Vijaykumar A, Robson P, Mina M. Single-cell transcriptome analysis defines mesenchymal stromal cells in the mouse incisor dental pulp. *Gene Expr Patterns* 2022; **43**: 119228 [PMID: 34915194 DOI: 10.1016/j.gep.2021.119228]

27   **Li J**, Wang Q, An Y, Chen X, Xing Y, Deng Q, Li Z, Wang S, Dai X, Liang N, Hou Y, Yang H, Shang Z. Integrative Single-Cell RNA-Seq and ATAC-Seq Analysis of Mesenchymal Stem/Stromal Cells Derived from Human Placenta. *Front Cell Dev Biol* 2022; **10**: 836887 [PMID: 35450295 DOI: 10.3389/fcell.2022.836887]

28   **Satija R**, Farrell JA, Gennert D, Schier AF, Regev A. Spatial reconstruction of single-cell gene expression data. *Nat Biotechnol* 2015; **33**: 495-502 [PMID: 25867923 DOI: 10.1038/nbt.3192]

29   **Kim S**, Kang D, Huo Z, Park Y, Tseng GC. Meta-analytic principal component analysis in integrative omics application. *Bioinformatics* 2018; **34**: 1321-1328 [PMID: 29186328 DOI: 10.1093/bioinformatics/btx765]

30   **Liberzon A**, Birger C, Thorvaldsdóttir H, Ghandi M, Mesirov JP, Tamayo P. The Molecular Signatures Database (MSigDB) hallmark gene set collection. *Cell Syst* 2015; **1**: 417-425 [PMID: 26771021 DOI: 10.1016/j.cels.2015.12.004]

31   **Yu G**, Wang LG, Han Y, He QY. clusterProfiler: an R package for comparing biological themes among gene clusters. *OMICS* 2012; **16**: 284-287 [PMID: 22455463 DOI: 10.1089/omi.2011.0118]

32   **Qiu X**, Hill A, Packer J, Lin D, Ma YA, Trapnell C. Single-cell mRNA quantification and differential analysis with Census. *Nat Methods* 2017; **14**: 309-315 [PMID: 28114287 DOI: 10.1038/nmeth.4150]

33   **Jin S**, Guerrero-Juarez CF, Zhang L, Chang I, Ramos R, Kuan CH, Myung P, Plikus MV, Nie Q. Inference and analysis of cell-cell communication using CellChat. *Nat Commun* 2021; **12**: 1088 [PMID: 33597522 DOI: 10.1038/s41467-021-21246-9]

34   **Fabian P**, Crump JG. Reassessing the embryonic origin and potential of craniofacial ectomesenchyme. *Semin Cell Dev Biol* 2023; **138**: 45-53 [PMID: 35331627 DOI: 10.1016/j.semcdb.2022.03.018]

35   **Colombo E**, Romaggi S, Medico E, Menon R, Mora M, Falcone C, Lochmüller H, Confalonieri P, Mantegazza R, Morandi L, Farina C. Human neurotrophin receptor p75NTR defines differentiation-oriented skeletal muscle precursor cells: implications for muscle regeneration. *J Neuropathol Exp Neurol* 2011; **70**: 133-142 [PMID: 21343882 DOI: 10.1097/NEN.0b013e3182084391]

36   **Mikami Y**, Suzuki S, Ishii Y, Watanabe N, Takahashi T, Isokawa K, Honda MJ. The p75 neurotrophin receptor regulates MC3T3-E1 osteoblastic differentiation. *Differentiation* 2012; **84**: 392-399 [PMID: 22906707 DOI: 10.1016/j.diff.2012.07.001]

37   **Yang K**, Wang Y, Ju Y, Li G, Liu C, Liu J, Liu Q, Wen X, Liu LC. p75 neurotrophin receptor regulates differential mineralization of rat ectomesenchymal stem cells. *Cell Prolif* 2017; **50** [PMID: 27672006 DOI: 10.1111/cpr.12290]

38   **Deng MJ**, Jin Y, Shi JN, Lu HB, Liu Y, He DW, Nie X, Smith AJ. Multilineage differentiation of ectomesenchymal cells isolated from the first branchial arch. *Tissue Eng* 2004; **10**: 1597-1606 [PMID: 15588419 DOI: 10.1089/ten.2004.10.1597]

39   **Zhang J**, Duan X, Zhang H, Deng Z, Zhou Z, Wen N, Smith AJ, Zhao W, Jin Y. Isolation of neural crest-derived stem cells from rat embryonic mandibular processes. *Biol Cell* 2006; **98**: 567-575 [PMID: 16719840 DOI: 10.1042/BC20060012]

40   **Wen X**, Liu L, Deng M, Zhang L, Liu R, Xing Y, Zhou X, Nie X. Characterization of p75(+) ectomesenchymal stem cells from rat embryonic facial process tissue. *Biochem Biophys Res Commun* 2012; **427**: 5-10 [PMID: 22982680 DOI: 10.1016/j.bbrc.2012.08.109]

41   **Liu Y**, Wang Z, Ju M, Zhao Y, Jing Y, Li J, Shao C, Fu T, Lv Z, Li G. Modification of COL1A1 in Autologous Adipose Tissue-Derived Progenitor Cells Rescues the Bone Phenotype in a Mouse Model of Osteogenesis Imperfecta. *J Bone Miner Res* 2021; **36**: 1521-1534 [PMID: 33950576 DOI: 10.1002/jbmr.4326]

42   **Malmgren B**, Andersson K, Lindahl K, Kindmark A, Grigelioniene G, Zachariadis V, Dahllöf G, Åström E. Tooth agenesis in osteogenesis imperfecta related to mutations in the collagen type I genes. *Oral Dis* 2017; **23**: 42-49 [PMID: 27510842 DOI: 10.1111/odi.12568]

43   **Boban I**, Jacquin C, Prior K, Barisic-Dujmovic T, Maye P, Clark SH, Aguila HL. The 3.6 kb DNA fragment from the rat Col1a1 gene promoter drives the expression of genes in both osteoblast and osteoclast lineage cells. *Bone* 2006; **39**: 1302-

1312 [PMID: 16938497 DOI: 10.1016/j.bone.2006.06.025]

44 **Long F**. Building strong bones: molecular regulation of the osteoblast lineage. *Nat Rev Mol Cell Biol* 2011; **13**: 27-38 [PMID: 22189423 DOI: 10.1038/nrm3254]

45 **Liao J**, Hu N, Zhou N, Lin L, Zhao C, Yi S, Fan T, Bao W, Liang X, Chen H, Xu W, Chen C, Cheng Q, Zeng Y, Si W, Yang Z, Huang W. Sox9 potentiates BMP2-induced chondrogenic differentiation and inhibits BMP2-induced osteogenic differentiation. *PLoS One* 2014; **9**: e89025 [PMID: 24551211 DOI: 10.1371/journal.pone.0089025]

46 **Goto N**, Fujimoto K, Fujii S, Ida-Yonemochi H, Ohshima H, Kawamoto T, Noshiro M, Shukunami C, Kozai K, Kato Y. Role of MSX1 in Osteogenic Differentiation of Human Dental Pulp Stem Cells. *Stem Cells Int* 2016; **2016**: 8035759 [PMID: 27648077 DOI: 10.1155/2016/8035759]

47 **Lin W**, Zhu X, Gao L, Mao M, Gao D, Huang Z. Osteomodulin positively regulates osteogenesis through interaction with BMP2. *Cell Death Dis* 2021; **12**: 147 [PMID: 33542209 DOI: 10.1038/s41419-021-03404-5]

48 **Chen J**, Wang N, Zhang H, Zhang X, Zhao L, Zhu L, Li Z, Bei C. [Lentivirus-mediated silencing of P75 neurotrophin receptor combined with nerve growth factor overexpression and transfection of bone marrow mesenchymal stem cells combined with demineralized bone matrix for heterotopic osteogenesis]. *Zhongguo Xiu Fu Chong Jian Wai Ke Za Zhi* 2020; **34**: 1438-1445 [PMID: 33191703 DOI: 10.7507/1002-1892.202003166]

49 **Wang Y**, Yang K, Li G, Liu R, Liu J, Li J, Tang M, Zhao M, Song J, Wen X. p75NTR(-/-) mice exhibit an alveolar bone loss phenotype and inhibited PI3K/Akt/β-catenin pathway. *Cell Prolif* 2020; **53**: e12800 [PMID: 32215984 DOI: 10.1111/cpr.12800]

50 **Shan P**, Wang X, Zhang Y, Teng Z, Jin Q, Liu J, Ma J, Nie X. P75 neurotrophin receptor positively regulates the odontogenic/osteogenic differentiation of ectomesenchymal stem cells *via* nuclear factor kappa-B signaling pathway. *Bioengineered* 2022; **13**: 11201-11213 [PMID: 35485233 DOI: 10.1080/21655979.2022.2063495]

51 **Rosset EM**, Bradshaw AD. SPARC/osteonectin in mineralized tissue. *Matrix Biol* 2016; **52-54**: 78-87 [PMID: 26851678 DOI: 10.1016/j.matbio.2016.02.001]

52 **Castro-Muñozledo F**, Meza-Aguilar DG, Domínguez-Castillo R, Hernández-Zequinely V, Sánchez-Guzmán E. Vimentin as a Marker of Early Differentiating, Highly Motile Corneal Epithelial Cells. *J Cell Physiol* 2017; **232**: 818-830 [PMID: 27404216 DOI: 10.1002/jcp.25487]

53 **Wang H**, Ning T, Song C, Luo X, Xu S, Zhang X, Deng Z, Ma D, Wu B. Priming integrin α5 promotes human dental pulp stem cells odontogenic differentiation due to extracellular matrix deposition and amplified extracellular matrix-receptor activity. *J Cell Physiol* 2019; **234**: 12897-12909 [PMID: 30556904 DOI: 10.1002/jcp.27954]

54 **Du C**, Li Y, Xia X, Du E, Lin Y, Lian J, Ren C, Li S, Wei W, Qin Y. Identification of a novel collagen-like peptide by high-throughput screening for effective wound-healing therapy. *Int J Biol Macromol* 2021; **173**: 541-553 [PMID: 33493562 DOI: 10.1016/j.ijbiomac.2021.01.104]

55 **Mantesso A**, Sharpe P. Dental stem cells for tooth regeneration and repair. *Expert Opin Biol Ther* 2009; **9**: 1143-1154 [PMID: 19653863 DOI: 10.1517/14712590903103795]

56 **Li G**, Liu J, Wang Y, Yang K, Zhao M, Xiao Y, Wen X, Liu L. LNGFR targets the Wnt/β-catenin pathway and promotes the osteogenic differentiation in rat ectomesenchymal stem cells. *Sci Rep* 2017; **7**: 11021 [PMID: 28887537 DOI: 10.1038/s41598-017-11555-9]